One-Step Synthesis of Bovine Serum Albumin Nanoparticles by Hydrothermal Green Treatment

Maghareh Esfahan, Zahra*+; Izhar, Shamsul
Department of Chemical & Environmental Engineering, Faculty of Engineering, University of Putra Malaysia, Selangor, 43400, MALAYSIA

Izadiyan, Zahra
Department of Chemistry, Faculty of Science, University of Malaysia, Kuala Lumpur, MALAYSIA

Toozandehjani, Meysam
New Technologies Research Center, Amirkabir University of Technology, Tehran Polytechnic, P.O. Box 15875-4413 Tehran, I.R. IRAN

Yoshida, Huroyuki
Department of Chemical & Environmental Engineering, Faculty of Engineering, University of Putra Malaysia, Selangor, 43400, MALAYSIA

ABSTRACT: *The non-toxic BSA-based NanoParticles (NPs) are developed without any additives with hydrothermal SubCritical Water Treatment (SCWT). The optimum BSA-based NPs are gained by applying Response Surface Methodology (RSM) based on particle size, zeta potential, and polydispersity. The SCWT conditions are optimized in terms of these three dependent variables, which have significant impacts on the BSA-based NPs application. The optimum BSA-based NPs prepared with 2.73% (w/v) of initial BSA solution concentration, the lowest initial concentration that is used to synthesize BSA-based NPs by now. The SCWT condition of 173 °C and 2.07 min of SCWT holding time shows that the zeta potential of -38.87 mV with the finest particle size and PI (147.32 nm and 0.24, respectively) is the optimized composition. The fabricated BSA-based NPs are characterized by the UV-vis, screening electron microscope (SEM), and stability assessment study.*

KEYWORDS: *Bovine serum albumin; Nanoparticle; hydrothermal; optimization; subcritical water treatment; green recovery; blood waste; drug delivery; response surface methodology.*

INTRODUCTION

Nanoparticles are produced with different types of components. The antigenic protein-based NPs are biocompatible, biodegradable, and easy to assemble [1,2]. The main protein of the vertebrate's plasma that is abundance in the slaughterhouse waste is Bovine Serum Albumin (BSA) with the M_w of 66 kDa; it is stable at a wide range

** To whom correspondence should be addressed.*
+ E-mail: shamizhar@upm.edu.my & zm.esfahan@yahoo.com
1021-9986/2023/6/1731-1743 13/$/6.03

of pH and does not have any structural changes by being heated up to 80 °C [3]. The clean and green hydrothermal technologies such as super/sub-critical treatment has been qualified for recovering the protein-rich feedstocks [4,5]. Due to the immunogenicity, nontoxicity, and biodegradability of albumin-based NPs, the formulated ones have the great potential to be used for drug delivery systems and it can be a great application of BSA waste recovery. Albumin NPs are synthesized by several techniques such as desolvation [6], nanospray drying [7], and NAB-technology [8]. Hydrothermal treatment with subcritical water technology is the recent technique used by researchers to synthesize nanopharmaceuticals because the use of organic solvents or chemicals led to undesirable results in previous methods [9–12]. Environmental pollution is an important issue and the high usage of organic solvents during these processes should be considered [13]. *Pu et al*. have been working on the substitution of SCW technology to conventional methods of producing nanoparticles. They used an organic solvent-free method, which would be a more economical and simpler treatment procedure in nanopharmaceuticals manufacturing processes [14–18]. By adjusting SCWT parameters and providing solvent anti-solvent precipitation conditions, protein-based nanoparticles have been synthesized successfully [16].

Response Surface Methodology (RSM) is mostly applied for reducing the number of experiments and optimizing experimental conditions in multivariate statistical techniques [19–21]. In this research, RSM was applied for optimum BSA-based NPs preparation conditions. This research aims to produce solvent-free and biocompatible BSA-based nanoparticles by using the SCWT method for the first time. Herein, we optimized the initial BSA solution concentration to reach the most miniature particles measurement, PDI less than 0.250, and surface charge lower than – 30 mV in BSA-based NPs [22,23].

EXPERIMENTS

BSA-based NPs preparation

BSA-based NPs were prepared by the nanoprecipitation concept, using the SCW approach that varies in the manner of the non-solvent. Initial BSA solution concentration was the main parameter that caused changes in the BSA-based biomaterial prepared under the hydrothermal condition. Various random reaction conditions were screened and then RSM was applied to determine the best condition of BSA-based NPs (Table).

Table 1: Experimental conditions of different BSA solution in SCWT.

Parameter	Range
Concentration % (w/v)	1–10
Reaction time (min)	0.5–15
Reaction temperature (°C)	80–200

Analysis of particle size, zeta potential, and PDI

The Nano ZS90 (Malvern, UK) was applied to determine the mean particle size (nm), zeta potential (mV), and PDI of the BSA-based NPs at room temperature. Diluted samples with deionized water (1: 100) were located in the capillary cell for the measuring process.

Design of experiments

The central composite rotatable designs (CCRD) with a five-level, three-factor approach was applied to investigate the influence of three independent factors such as initial BSA concentration (x_1) (1.32–4.68%, w/v), SCWT temperature (x_2) (159.77-210.23°C), and SCWT holding time (x_3) (0.46–9.29min) on the dependent factors (particle size (Y_1), zeta potential (Y_2), and PDI (Y_3)). By applying "Design Expert-11", 20 runs were set up, which included eight factorial, six axial, and six repeated conditions. Optimization was done to obtain SCWT conditions to control the particle size, zeta potential magnificent, and PDI. Table 2**:** shows all five different coded independent variables. The CCRD method provides the possibility of simultaneous interpretation of non-dependent variables and independent variables interaction on the results.

Characterization

UV-Vis absorption

The UVs absorption spectra is calculated shortly after the preparation of BSA-based NPs, using the wavelength range of 400-800 nm by employing the UV-Vis spectrophotometer (UV-1800, SHIMADZU).

Screening Electronic Microscopy (SEM)

The surface formation and changes of BSA-based NPs samples were scrutinized by screening electronic microscopy.

Table 2: Independent parameters for RSM design application.

Variables	Unit	Symbol	Levels				
			-α	-1	0	+1	+α
Initial BSA solution concentration	(w/v)	X_1	1.32	2	3	4	4.68
SCW-temperature	(°C)	X_2	159.77	170	185	200	210.23
SCW-time	(min)	X_3	0.46	2.25	4.88	7.5	9.29

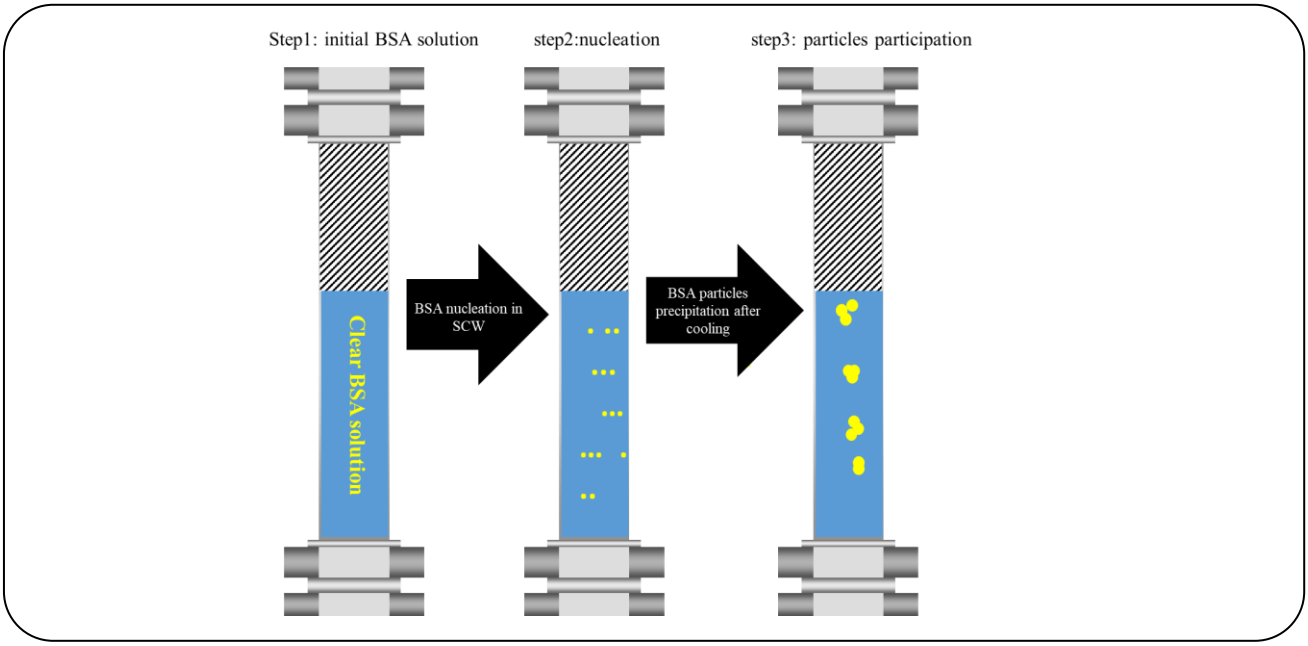

Scheme 1: Schematic diagram of BSA particles formation during SCWT.

The NPs surface size distributions were detected by using the Hitachi S-3400N Tabletop Microscope.

Stability test

Investigation of BSA-based NPs stability was measured by monitoring the main factors such as particles size and color changes and precipitation during the storage in different duration. Freshly prepared samples of BSA-based NPs were put into test tubes. The mean particle size, zeta potential, and PDI of BSA-based NPs were measured to investigate varying changes over the time after one week, a month, and three months.

RESULTS AND DISCUSION

Formation of BSA-based NPs by SCWT

BSA is dissolved in a liquid phase, whereas SCW is applied as a low-grade solvent for proteins with excellent water solubility. Afterward, under the optimum condition of the temperature and pressure, the supersaturated BSA nucleus was formed in the hydrothermal reactor. This is followed by the condensation of the BSA units around the nucleus to produce BSA-based NPs (Scheme 1). The precipitation technique was used to prepare size-controlled BSA-based NPs and unimodal distribution [24,25].

Screening the independent parameters

A research was conducted to assess the percentage of independent factors. According to the outcomes, the lower, central, and higher levels of the three independent factors were obtained. The initial ranges were selected based on the preliminary studies**.** Protein-based NPs used in drug delivery systems should have particle sizes of less than 150 nm, PDI about 109.0.1-0.270, and zeta potential of ± 25 mV. These ranges were used for the optimization study to determine the optimum condition. Other SCWT parameters, such as heating bath string speed and cooling time, were fixed because their effects on the modeling framework are negligible [26].

Table 3: The predicted and experimental sets of particle size, zeta potential, and PDI design by CCRD.

Run	X1	X2	X3	Particle size		Zeta Potential		PDI	
				Actual	Predicted	Actual	Predicted	Actual	Predicted
1	2.00	200.00	7.50	145.10	145.10	-32.70	-32.56	0.13	0.11
2	3.00	185.00	9.29	371.60	371.60	-40.30	-40.68	0.40	0.42
3	3.00	210.23	4.88	8799.00	8799.00	-23.60	-23.84	0.73	0.76
4	2.00	170.00	7.50	603.30	603.30	-19.80	-20.04	1.00	0.98
5	2.00	170.00	2.25	253.90	253.90	-33.40	-33.40	0.32	0.34
6	3.00	185.00	4.88	408.00	408.00	-12.20	-12.06	0.51	0.48
7	4.00	200.00	7.50	972.10	972.10	-26.00	-26.38	1.00	0.98
8	3.00	159.77	4.88	480.50	480.50	-25.50	-25.16	1.00	1.02
9	4.00	170.00	7.50	3755.00	3755.00	-30.40	-30.23	0.72	0.63
10	3.00	185.00	4.88	414.30	468.66	-33.40	-33.23	0.78	0.69
11	4.68	185.00	4.88	4260.20	4800.56	-36.60	-36.43	0.47	0.47
12	3.00	185.00	0.46	350.00	3755.00	-36.30	-36.13	1.00	1.00
13	3.00	185.00	4.88	569.90	468.66	-34.00	-30.78	0.43	0.43
14	3.00	185.00	4.88	608.50	480.56	-28.10	-30.78	0.59	0.59
15	1.32	185.00	4.88	400.00	474.61	-28.50	-30.78	0.80	0.66
16	2.00	200.00	2.25	573.80	474.61	-30.00	-30.78	0.53	0.66
17	4.00	170.00	2.25	454.20	474.61	-28.80	-30.78	0.53	0.66
18	3.00	185.00	4.88	145.10	174.61	-35.20	-30.78	0.60	0.66
19	3.00	185.00	4.88	371.60	474.61	-32.70	-32.56	0.67	0.66
20	4.00	200.00	2.25	499.00	474.61	-40.30	-40.68	0.69	0.66

**Note: X_1 (initial concentration, g/mL), X_2 (temperature, °C), X_3 (time, min)*

Fitting the response surface models and statistical analysis

The actual and predicted values are shown in Table 3 Based on the experiments, models are chosen quadratic, quadratic, and linear for particle size, zeta potential, and PDI respectively. The synthesized BSA-based NPs illustrated a particle size, zeta potential, and PDI within the range of 145.10 to 8799.00 nm, -12.06 to -40.68mV, and 0.11 to 1.02, respectively. The CCRD provided a model to estimate variations of dependent factors as a function of SCWT conditions.

Analysis of variance (ANOVA) showed that the SCW-temperature (X_2) and initial BSA concentration, X_1, with a great F-value (500.53, 26.80) and acceptable p-value (< 0.0001) was the most significant parameter affecting the BSA-based particle size and zeta potential. Additionally, in the linear prediction model of the PDI, the concentration of the initial BSA solution (w/v) was the most influential factor with (P-value<0.001, F-value =14.63).

The combination of high F-values and low P-values revealed remarkable consequences about the individual response parameters [27]. Moreover, the ANOVA results recommended the quadratic model for particle size and zeta potential as well as a linear model for PDI prediction, and they received the highest coefficient correlation (R^2 = 0. 9992, 0. 9306, 0. 9381), respectively.

In this study, SCWT was employed for synthesizing BSA-based NPs from BSA solution to assess if they can be used as an alternative and novel method without using any reagent, toxic cross-linker, and organic solvent-free

and within a shorter processing time to prepare the BSA-based NPs. Response surface methodology is used to find the best operating condition for BSA-based NPs preparation. Conclusively, based on the assumptions of RSM (Table 3), the mathematical models for prediction of Particle Size (PS), Zeta Potential (ZP), and PDI are represented in equation 1 to 3 respectively.

$$PS(nm) = 474.61 - 1174.09X_1 + 973.51X_2 + 3.54X_3 - 1143.36\,X_1X_2 + 1371.95X_1X_3 - 81.59X_2X_3 + 874.01X_1^2 + 580.94\,X_2^2 + 1515.92X_1X_2X_3 + 612.56\,X_1^2X_2 \quad (1)$$

$$ZP\ (Y_2) = -30.78 - 5.61\,X_1 - 0.89X_2 + 0.089X_3 - 0.24X_1X_2 - 1.31X_1X_3 - 0.18X_2X_3 + 5.32X_1{}^2 - 0.34X_2{}^2 - 1.95\,X_3^2 + 4.83\,X_1^2X_2 + 4.68\,X_2^2X_3 \quad (2)$$

$$PDI(Y_3) = +0.66 + 0.018X_1 + 0.16X_2 + 0.047X_3 - 0.023\,X_1X_2 - 0.043\,X_1X_3 - 3.750e^{-}003X_2X_3 + 0.025\,X_2^2 - 0.054\,X_3^2 + 0.072X_1X_2^2 + 0.023\,X_2^2X_3 + 0.14\,X_2X_3^2 \quad (3)$$

Response surface analysis

Average particle size (nm)

Three-dimensional (3D) graphs show the effect of initial BSA solution concentration, SCW temperature, and SCW holding time in Fig. 1(a); the increase in SCW temperature negatively affected the average particle size. Conversely, the increase of the initial BSA concentration was an effective factor in the response value (Fig. 1(b)). This behavior may be explained by a better precipitation condition provided at a higher initial BSA concentration. While the initial BSA concentration was the most meaningful effective factor for the particle size of BSA-based NPs, the time of SCW did not have an effect on this response notably (Fig. 1(c)). The ideal mean particle size was derived from the combination of 2.73% (w/v) BSA, 173°C, and 2.07 min.

During hydrothermal diffusion, BSA molecules overcome its thermodynamic water-soluble region, and the system commences to form the protein NPs nuclei. It means that, development of the BSA-based NPs depends on the pH of the process that in this system is controlled by the initial BSA concentration and SCW temperature. If the pH is not sufficient to meet the supersaturation state,

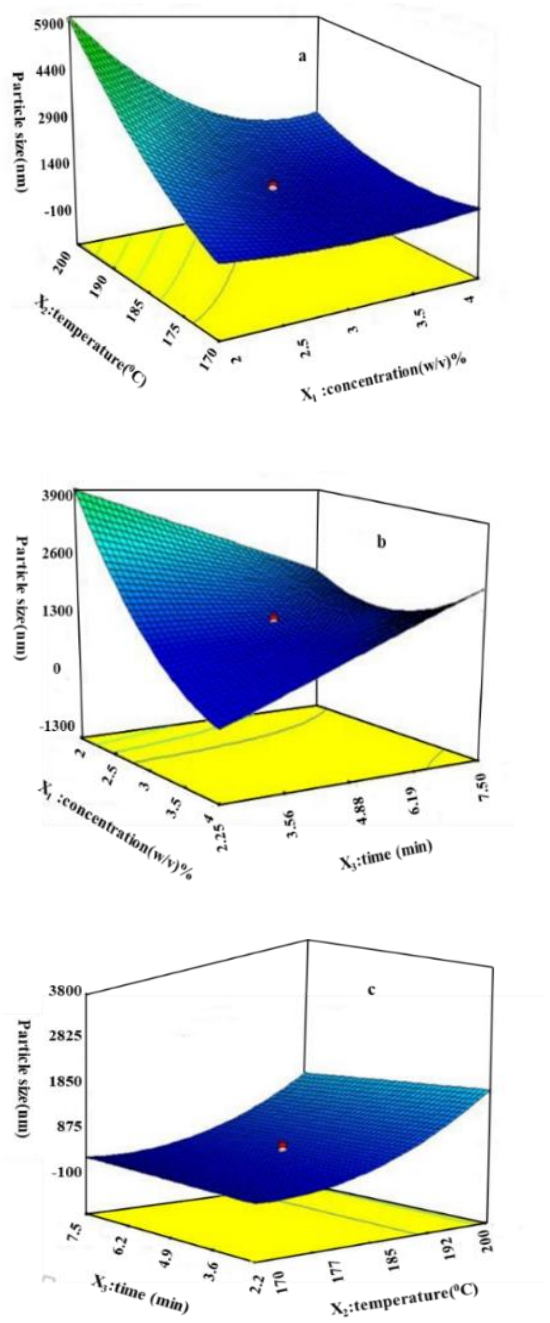

Fig. 1: Response surface diagrams for mean particle size (nm) as a function of (a) initial BSA concentration, (b) preparation temperature and(c) time.

precipitation does not increase or results in irregular particles with a wide range of particle size distribution. This could be explained by the size interruption at the lower SCW temperature. Simply, the temperature was as low as possible to achieve proper precipitation. It was found that for an initial BSA solution concentration of

2-2.5% (w/v) BSA and SCW temperature of 170 ºC, BSA-based NPs with uniformed size distribution were detected and narrowed by decreasing SCW temperature. However, a little coagulation is .occurred in the reparation sample at 173 °C.

The results showed when the SCW temperature was above 175 ºC, the particle size distribution would be wide, and the measurement would be awkward. These results were found in the same line with [28]. The BSA concentration influences the zeta potential of NPs, which has been evaluated. This result is in agreement with previous works on the preparation of human serum albumin (HSA) NPs by nanoprecipitation [6,22,29]. They reported that the HAS concentration in the range of 25 to 100 mg/mL has no notable effect on the particle size (particle size varied from 150 to 170 nm). On the other hand, in the newer research, initial BSA concentration increment from 12 to 100 mg/mL doubled the particle size (75 increased to 135 nm). In contrast, it was revealed that the BSA concentration increase between 5 to 30 mg/mL caused the particle size reduction of 204 to 145.7 nm [25].

Zeta potential

Fig. 2(a) shows that by increasing the initial BSA concentration, the zeta potential of BSA-based NPs decreased to -31mV around 2.5% (w/v) of the initial BSA concentration and then increased by increasing the initial BSA concentration. In contrast, SCW temperature changes had the opposite effect on zeta potential. It means that by increasing SCW temperature from 170°C to around 185 °C, the zeta potential of BSA-based NPs increased from -35 mV to -32 mV. Above 185 °C, by increasing SCW temperature, the zeta potential was decreased to -40 Mv (Fig. 2(b)). As the results reveal, BSA-based NPs produced by SCW under mild conditions showed a decrease in negative surface load compared to BSA-based NPs produced in the upper and down limits of SCW condition. The holding time also did not have a significant influence on the zeta potential (Fig. 2(c)).

The zeta potential value decreased by increasing the SCW temperature, and then it increased to a maximum of 2.5% (w/v). It could be explained that samples are spread extremely, and then at elevated SCW temperature, it is not measured accurately. Besides, it is believed that the great absolute zeta potential content leads to the excellent colloidal durability of NPs. As shown in Fig. 2(b), BSA-based NPs had the greatest colloidal stability at the initial BSA concentration of 2 %(w/v).

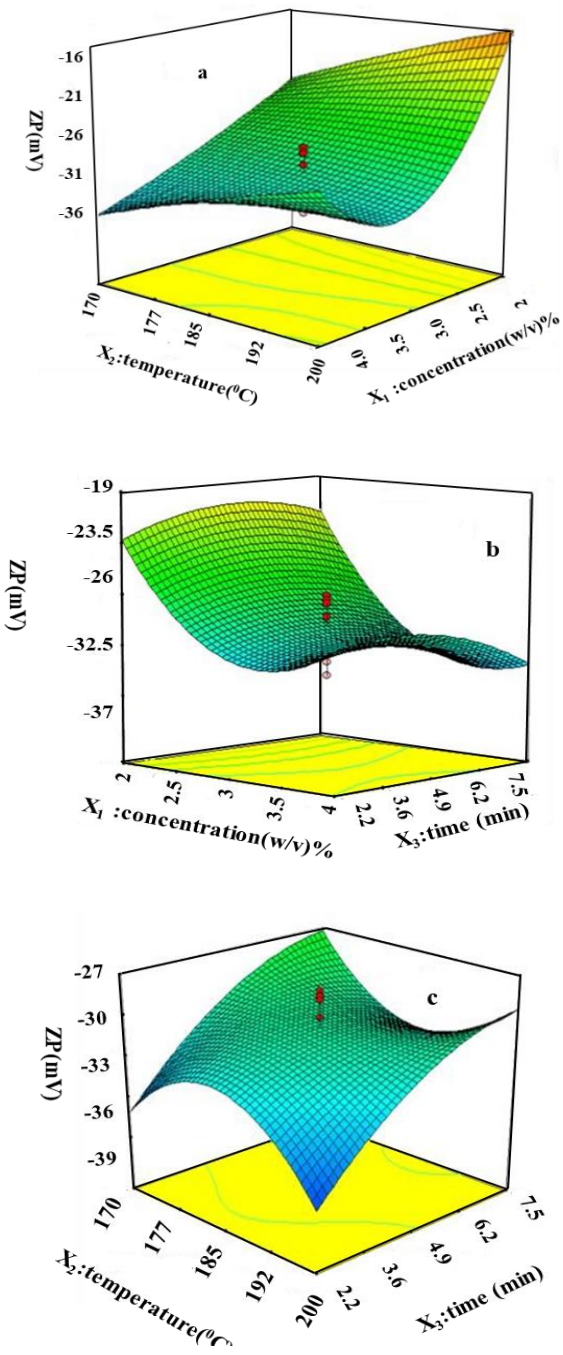

Fig. 2: Response surface diagrams for the mean zeta potential as a function of (a) initial BSA concentration, (b) preparation temperature, (c) time.

Polydispersity index (PDI)

Fig. 3(a) indicates that the maximum PDI associated with the highest SCW condition (i.e., 200 °C, 7.5 min

and 4% (w/v) initial BSA concentration) is not within the acceptable range of NPs for medicinal applications, while the SCW temperature decreased to 170 °C and the reaction time to 2.25 min (Fig. 3(b)) and the PDI decreased sharply to around 0.25. However, the results indicated a wide variation in PDI due to a small change in SCW temperature, while PDI with an initial BSA concentration changed slightly. The optimum PDI obtained at the set level of 2.73% (w/v) BSA, 173 °C, 2.07 min determined using the response surface diagrams (lowest PDI value, Y_3=0.253).

However, a small amount of particles coagulation appeared in samples that have been processed above 170 °C. In addition, when the SCWT holding time was around 5 min, the peak lost its perfect Gaussian shape and switched to the left, demonstrating a rise in PDI. A narrow peak illustrating the presence of coagulation was also detected **(Figure 3(b))**. Eventually, at a holding time of 5 min, an unusual peak indicated the high PDI of the BSA-based particles with a strong association (Fig. 3: c)).

In this research, it was approved that the experimental factors of the nanoparticles precipitation method could have a dramatic effect on the colloidal properties of NPs. Besides, the change of experimental factors can increase PDI in the samples. The highest concentration of bovine serum albumin can considerably influence the capability of emulsification. In this case, the coalescence rate increased sharply. Therefore, bigger particles tend to aggregate in a shorter time compared to small particles, and broader particle size distribution leads to higher PDI [30].

Optimization of operational condition

The optimum condition refers to the condition in which SCW treatment has produced the best BSA-based NPs in terms of particle size, zeta potential, and PDI. The RSM results indicated that the optimum SCW parameters were as follows: temperature of 173 °C, initial BSA concentration of 2.73% (w/v), and SCW time of 2.07 min. Response values (i.e., particle size, zeta potential, and PDI) under the optimum conditions can be found in Table 4. The optimal condition of BSA-based NPs resulted in 146.398 nm, -39.5161 mV, and 0.239, respectively, for particle size, zeta potential, and PDI. Given the similarity of the experimental data and predicted values, the model was approved. The conclusion was that the experimental model

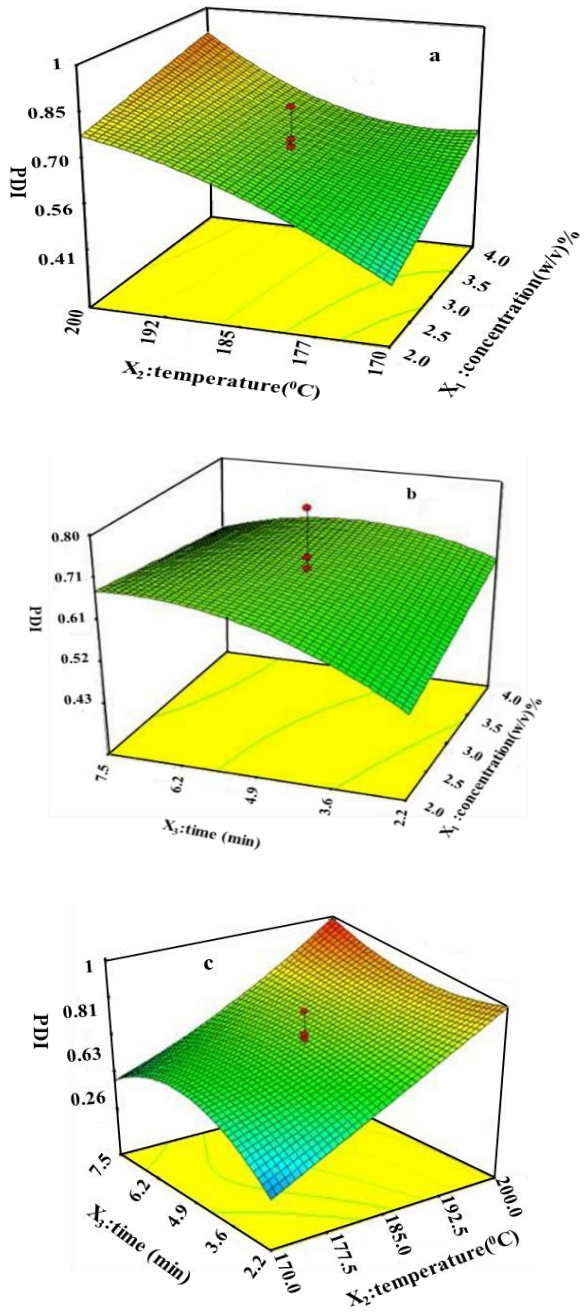

Fig. 3: Response surface diagrams for average PDI as a function of (a) initial BSA concentration, (b) SCWT-temperature, (c) SCWT holding time.

by RSM design could sufficiently explain the dependency degree of effective factors and responses.

BSA-based NPs have been prepared under various SCW treatment conditions. It was clear from visually inspected specimens that there was a variance in the properties of BSA-based NPs at varying SCW temperatures.

Table 4: The optimum condition derived by RSM For SCW preparing BSA-based Nps.

Optimum conditions			Responses					
X_1^*	X_2^*	X_3^*	Particle Size(nm)		Zeta Potential(mV)		PDI	
			Actual	Predicted	Actual	Predicted	Actual	predicted
173 °C	2.73	2.07	147.02	146.398	-38.87	-39.52	0.24	0.239

$^*X_1$= temperature (°C), X_2= initial BSA solution concentration %(w/v), X_3= SCW time (min)

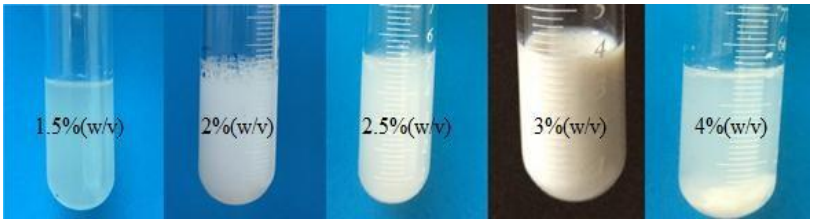

Fig. 4: BSA-based NPs prepared in different initial BSA solution concentrations by SCW.

Samples produced in the 170°C range exhibited a transparent white color. By increasing the initial BSA concentration, the color (i.e., opacity) of the suspension solution became whiter and more stable until it ceased to be transparent at 2.5% (w/v) initial BSA concentration (Fig. 4). It can be assumed that the self-assembly process is also used in the preparation of BSA-based NPs using the SCW method by increasing the initial BSA concentration in addition to the precipitation. Increasing the hydrophobicity of albumin and primary amine groups on the protein surface could lead to the self-assembly of BSA-based stable suspension. The formation of the inner core was a combination of albumin via disulfide bonds, resulting in the formation of multimeric albumin aggregates. The result is the production of very stable BSA-based NPs with a very good surface charge.

Characterization

Formation of BSA-based NPs analysis by UV-vis

The UV-visible spectra of pure BSA and BSA-based NPs prepared at optimum SCW condition (173 °C, 2.73% (w/v) initial BSA and 2.07 min). The maximum absorption peaks were evaluated between 220 and 400 nm. Fig. 5(a) shows that raw BSA powder had two absorption peaks at 209 and 278 nm associated with the absorption of aromatic amino acids (orange line) and the optimum BSA-based NPs at room temperature (blue line). It shows the improvement in absorption before 280 nm. Due to the capability of the BSA to offer multiple connection sites, which may consist of the –NH, –SH, –COOH, and –OH groups, the absorption peak moved to a right (red shift) wavelength of approximately 212 nm after SCWT.

Fig. shows the UV spectra of BSA-based NPs synthesized in different initial BSA concentration solutions at optimum SCW temperature and time. According to the UV spectra, the special absorption peaks of BSA-based NPs appeared at the same site (192 nm). The particle size has a direct effect on the absorption intensity and peak width [31,32]. Based on this principle, it can be concluded that the size of BSA-based NPs is maximum in 2.73 mg/mL BSA solution and that the size of BSA-based NPs is minimum in 4.5 mg/mL (no NPs) BSA solution. These findings are consistent with the predicted RSM result concerning the impact of initial BSA concentration on the initial experiments. It was found that the solution color (after the SCW precursor) had shifted from transparency to white opacity stable emulsion by increasing the initial BSA concentration. Moreover, at concentrations of more than 4% (w/v), the stable white emulsion disappeared with the formation of two phases of transparent liquid and white solid.

When BSA-based NPs were formulated, the intensity of the peak was decreased. These results indicated that the formation of BSA-based NPs altered BSA backbone amino acids by maintaining aromatic amino acids for drug interaction [33].

These sites include most molecular amino acids that may bind to hydrophobic or positively charged surfaces. Thus, there is a great possibility of the direct interaction of these subdomains with negatively charged molecules

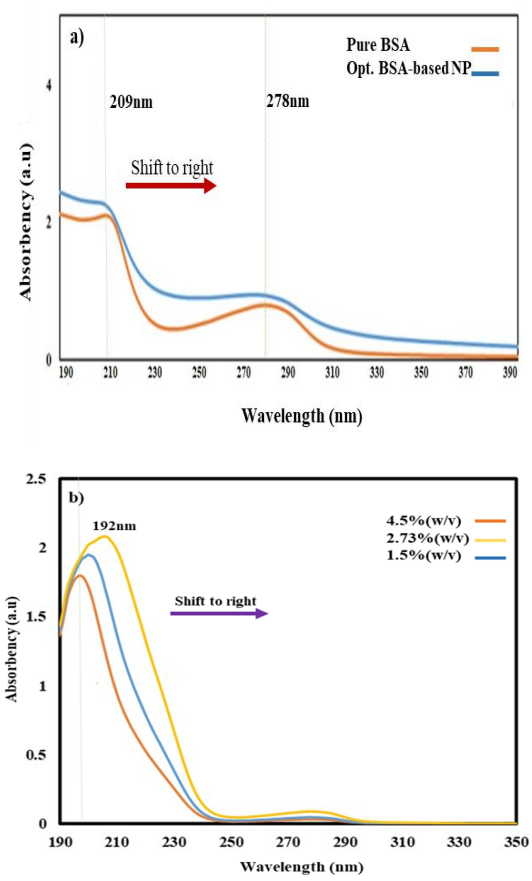

Fig. 5: UV–vis absorption spectra for a) BSA solution and optimum BSA-based NP prepared at 173 ℃, 2.73 (w/v) % and 2.07min, b) BSA-based NPs prepared at concentration of 4.5 %(w/v),1.5 %(w/v), 2.73 %(w/v)

or delocalized negative charges like heterocyclic ligands or carboxylic acids [33]. The outcome of UV-*Vis* spectroscopy is strongly supported by other synthetic BSA-based NPs [22,34,35].

Structural analysis and particle size distribution of opting BSA-based NPs

Fig. 6 (a) illustrates SEM images of biosynthesized BSA-based NPs with initial BSA concentrations of 1.5, 2.73, and 4.5% (w/v) via SCW. The SEM images and their size distribution indicated that the mean diameters and standard deviation of BSA-based NPs were around 100-110 nm at room temperature, as shown in Fig. 6(b). These SEM results are in agreement with the RSM optimization and UV–vis results. Fig. 6(c) shows the stable BSA nanoemulsion from 2.73% (w/v) initial BSA solution and an increase of the initial BSA concentration to more than 4.5% (w/v) of the NPs. According to the preparation section, no BSA-based NPs were formed at the initial BSA 1.5% (w/v) concentrations due to the lack of BSA molecules to complete in the three steps. BSA-based NPs exhibited a zeta potential of -36.1 mV, which is good for stable nanosuspension. In line with the results of the particle size analysis, SEM images suggested that the shape of the NPs is almost spherical and monodisperse without aggregates. SCW agrees with the particle size of BSA-based NPs and the result of BSA-based NPs prepared by using pH 7 and 2 mM of ionic strength (time consuming and using toxic chemicals) [36].

The BSA NPs have been prepared as a colloidal carrier in the presence of glutaraldehyde in the range of 101–503 nm [37], while those for drug or nutrient carriers were 400–820 nm for an anti-tumor 5-fluorouracil carrier [38] and 50–400 nm for a bone morphogenetic protein carrier [39]. Malvern assessed different BSA-based NPs size distributions from different initial BSA concentrations to determine the amount of BSA needed to prepare NPs with sufficient sizes.

The particle size distribution of the prepared NPs is shown in Fig. 7. For BSA protein, the optimum initial concentration of 2.73% (w/v) was achieved by RSM software as the desired concentration of BSA for NPs with a target size of drug delivery application. The optimum size was not produced in the higher and lower SCW condition (i.e. temperature and holding time) as shown in UV-vis and SEM. Galisteo-Gonzalez and Molina-Bolivar (2014) reported that BSA-based NPs with a size of 100–120 nm were derived from the desolvation method in the presence of glutaraldehyde in 8 h. Besides, the results of the earlier studies indicated that for the preparation of BSA NPs, the level of protein should be between 50 and 60 g/L. However, in the green SCW preparation method used for the first time in this study, a lower concentration of BSA prepared BSA-based NPs with a diameter of 100-200 nm.

Zeta potential analysis

The zeta potential analysis was performed to collect information on the surface properties of the BSA-based NPs. The stability of systems can be demonstrated in the long term by this analysis. A zeta value of about ±25 mV is required for a physical suspension stabilized by electrostatic repulsion [40].

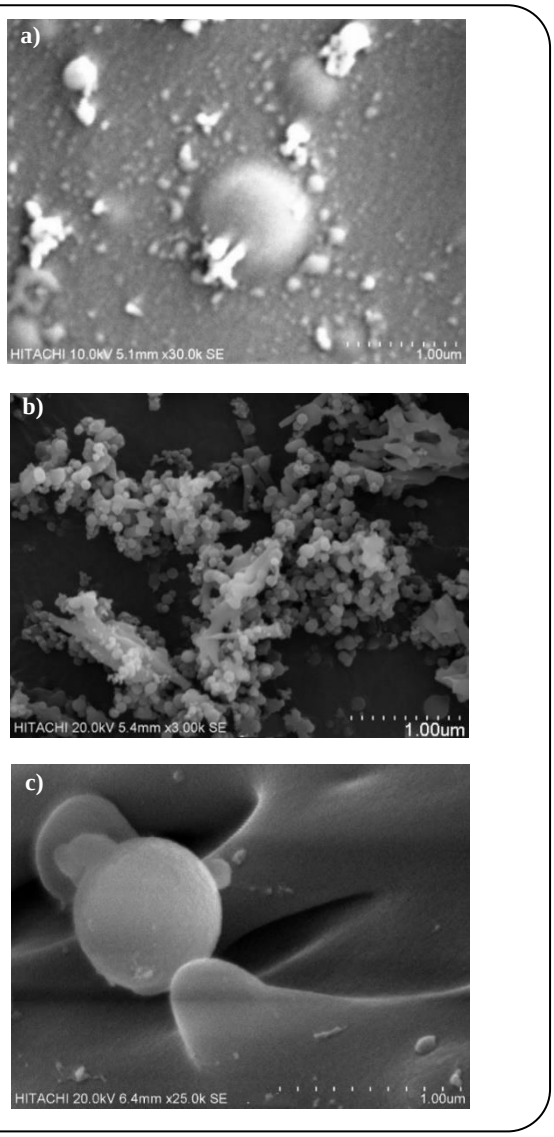

Fig. 6: Representative images for (a) BSA-based NPs prepared with 1.5%(w/v)initial BSA solution concentration, (b) BSA-based NPs prepared with 2.73%(w/v)initial BSA solution concentration, and (c) BSA-based NPs prepared with 4.5%(w/v)initial BSA solution concentration.

The negative zeta potential (-38.87 mV) for BSA-based NPs shows that a high absolute zeta potential value implies high colloidal stability of NPs [41]. Based on the adequate value for solution stability (±25 mV) [42], the BSA-based NPs were sufficiently stable.

BSA-based NPs stability test

To check the short-term stability of BSA-based NPs, it was centrifuged for 15min, 45min and 60 min. There was not any changes in the emulsion appearance. Particle size,

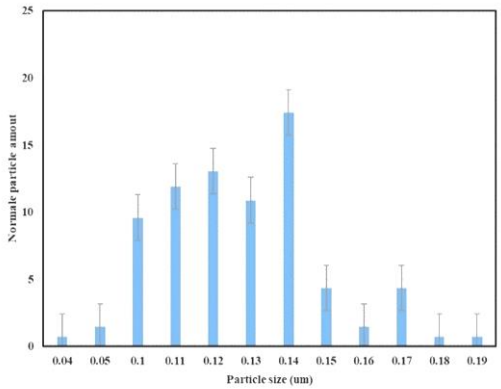

Fig. 7: Particle size distribution of BSA-based NPs which prepared at 173°C, 2.07min and 2.73% (w/v) initial BSA, (327 particles counted).

PDI and zeta potential have a significant role to play in assessing the stability of the nanoparticles in long term storage. The result of their long-term changes is listed in Table 5.

A drastic dependence of colloidal properties of BSA-based NPs with experimental factors has been confirmed. Particle size, zeta potential, and PDI were obtained by Zetasizer and provided in Over the three months, the particle size, PDI, and zeta potential of BSA-based NPs were found to be stable with no remarkable changes. In general, this will lead to faster aggregation. Large particles tend to coalesce faster than small particles. Each droplet is surrounded by a shear-plane potential called zeta potential. Repulsive electrostatic interactions between emulsion droplets with a similar charge prevent them from getting closer and thus preventing coalescence [43]. The change in zeta potential over time is the result of an increase or decrease in the surface charge of particles. Earlier reports indicate that the fabricated BSA-based NPs are negatively charged and stabilized by electrostatic repulsion [44]. Furthermore, more considerable surface potential leads to more active repulsion between colloidal particles, resulting in more moderate coagulation kinetics corresponding to observation [45]. PDI provides information on the deviation from the average size between large and small particles.

CONCLUSIONS

For the first time, the BSA-based NPs were synthesized with SCWT technology. The influence of the important

Table 5: The long-term stability test result of BSA-based NPs by SCW.

Time (week)	Particle size (nm)	Zeta potential (mV)	PDI
0	147.02	-39.52	0.240
1	147.1	-39.5	0.253
4	146.15	-39.28	0.259
12	146.35	-38.81	0.259

factors on the particle size and colloidal properties of BSA-based NPs has been studied. BSA-based NPs were produced without using cross-linkers or any toxic chemicals with unimodal particle size distribution depending on the variation of the experimental factors in a very short time. Besides, the initial BSA concentration may have a dramatic effect on the particles size and zeta potential. On the other hand, some factors may cause coagulation or dissociation of the prepared particles due to instability. This research was capable of identifying the optimal conditions for the producing of BSA-based NPs using the SCW method, which could be an excellent candidate for *in vivo* drug delivery since no toxic additives were used in the formation process.

Nomenclatures

BSA	Bovine Serum Albumin
SCWT	Subcritical Water Treatment
NPs	Nanoparticles
ZP	Zeta Potential
PDI	Polydispersity Index

Acknowledgments

The authors would like to acknowledge the support given by Assoc. Prof. Mohd Razif Harun and Dr. Mohd Halim Shah Ismail. I regret to state that Dr. Mohd Halim Shah Ismail passed away on 18 August 2020. Let us wish so that he will be granted a good place in the afterlife.

Received : Jul 22, 2022 ; Accepted : Oct. 10, 2022

REFERENCES

[1] Vauthier C. and Ponchel G., "Polymer Nanoparticles for Nanomedicies", 1st ed., Springer International Publishing, (2016).

[2] Barros C.H.N., Casey E., A Review of Nanomaterials and Technologies for Enhancing the Antibiofilm Activity of Natural Products and Phytochemicals, *ACS Appl. Nano Mater.*, **3**: 8537 (2020).

[3] Esfahan Z.M., Izhar S., Shah Ismail M.H., Hiroyuki Y., Subcritical Water Treatment of Bovine Serum Albumin Pathway to Produce Superabsorbent Biomaterial as Green Technology, *Mater. Today Sustain*, 100087 (2021).

[4] Stablein M.J., Aierzhati A., Watson J., Si B., Zhang Y., Characterization and Bioremediation Potential of Byproducts from Hydrothermal Liquefaction of Food Wastes, *Bioresour Technol Reports*, **12**: 100555 (2020).

[5] Cheng Y., Xue F., Yu S., Du S., Yang Y., Lovillo M.P., et al., "Subcritical Water Extraction of Natural Products", Mol 2021, Vol 26, Page 4004, **26**: 4004 (2021).

[6] Jahanban-Esfahlan A., Dastmalchi S., and Davaran S., A Simple Improved Desolvation Method for the Rapid Preparation of Albumin Nanoparticles, *Int. J. Biol. Macromol.*, **91**: 703 (2016).

[7] Lee S.H., Heng D., Ng W.K., Chan H.-K., Tan R.B.H., Nano Spray Drying: A Novel Method for Preparing Protein Nanoparticles for Protein Therapy, *Int. J. Pharm.*, **403**: 192 (2011).

[8] Luo H., Sheng J., Shi L.L., Yang X., Chen J., Peng T., et al., Non-Covalent Assembly of Albumin Nanoparticles by Hydroxyl Radical: A Possible Mechanism of the Nab Technology and a One-Step Green Method to Produce Protein Nanocarriers, *Chem. Eng. J.*, **404**: 126362 (2021).

[9] Pu Y., Wang J.X., Wang D., Foster N.R., Chen J.F., Subcritical Water Processing for Nanopharmaceuticals, *Chem. Eng. Process - Process Intensif*, **140**: 36 (2019).

[10] Machmudah S., Widiyastuti W., Wahyudiono W., Winardi S., Kanda H., Goto M., Hydrothermal Synthesis: Low−Temperature Subcritical Water for Ceria−Zirconia Mixed Oxides Preparation, *Indones. J. Chem.*, **21**: 1 (2021).

[11] Mohammadi H.S., Asl A.H., Khajenoori M., Solubility Measurement and Preparation of Nanoparticles of Ampicillin Using Subcritical Water Precipitation Method, *Korean J. Chem. Eng.*, **2021**: 1 (2021).

[12] Parmentier M., Gabriel C.M., Guo P., Isley N.A., Zhou J., Gallou F., Switching from Organic Solvents to Water at an Industrial Scale, *Curr. Opin. Green Sustain. Chem.*, **7**: 13 (2017).

[13] Cseri L., Razali M., Pogany P., Szekely G., "Organic Solvents in Sustainable Synthesis and Engineering", Green Chem. An Incl. Approach, Elsevier Inc., 513 (2018).

[14] Fattahi A., Karimi-Sabet J., Keshavarz A., Golzary A., Rafiee-Tehrani M., Dorkoosh F.A., Preparation and Characterization of Simvastatin Nanoparticles Using Rapid Expansion of Supercritical Solution (RESS) with Trifluoromethane, *J. Supercrit Fluids*, **107**: 469 (2016).

[15] Sodeifian G., Sajadian S.A., Solubility Measurement And Preparation of Nanoparticles of an Anticancer Drug (Letrozole) Using Rapid Expansion of Supercritical Solutions With Solid Cosolvent (RESS-SC), *J. Supercrit Fluids*, **133**: 239 (2018).

[16] Pu Y., Li Y., Wang D., Foster N.R., Wang J.-X., Chen J.-F., A Green Route to Beclomethasone Dipropionate Danoparticles Via Solvent Anti-Solvent Precipitation by Using Subcritical Water as the Solvent, *Powder Technol*., **308**: 200 (2017).

[17] Pu Y., Wen X., Li Y., Wang D., Foster N.R., Chen J.-F., Ultrafine Clarithromycin Nanoparticles Via Anti-Solvent Precipitation In Subcritical Water: Effect of Operating Parameters, *Powder Technol.*, **305**: 125 (2017).

[18] Abbasi Kajani A., Haghjooy Javanmard S., Asadnia M., Razmjou A., Recent Advances in Nanomaterials Development for Nanomedicine and Cancer, *ACS Appl Bio Mater*, **4**: 5908 (2021).

[19] Mozdianfard M.R., Masoodiyeh F., Karimi-Sabet J., Supercritical Water Hydrothermal Synthesis of Bi_2O_3 Nanoparticles: Process Optimization Using Response Surface Methodology Based on Population Balance Equation, *J. Supercrit Fluids*, **136**: 144 (2018).

[20] Mohtashamian S., Boddohi S., Hosseinkhani S., Preparation and Optimization of Self-Assembled Chondroitin Sulfate-Nisin Nanogel Based on Quality By Design Concept, *Int. J. Biol. Macromol.*, **107**: 2730 (2018).

[21] Gundupalli M.P., Tantayotai P., Panakkal E.J., Chuetor S., Kirdponpattara S., Thomas A.S.S., et al., Hydrothermal Pretreatment Optimization and Deep Eutectic Solvent Pretreatment of Lignocellulosic Biomass: an Integrated Approach, *Bioresour Technol. Reports.*, **17**: 100957 (2022).

[22] Bronze-Uhle E.S., Costa B.C., Ximenes V.F., and Lisboa-Filho P.N., Synthetic Nanoparticles of Bovine Serum Albumin with Entrapped Salicylic Acid, *Nanotechnol Sc.i Appl.*, **10**: 11 (2017).

[23] Yedomon B., Fessi H., Charcosset C., Preparation of Bovine Serum Albumin (BSA) Nanoparticles by Desolvation Using a Membrane Contactor: A New Tool for Large Scale Production, *Eur. J. Pharm. Biopharm.*, **85**: 398 (2013).

[24] D'Addio S.M., Prud'homme R.K., Controlling Drug Nanoparticle Formation by Rapid Precipitation, *Adv. Drug. Deliv. Rev.*, **63**: 417 (2011).

[25] Tarhini M., Benlyamani I., Hamdani S., Agusti G., Fessi H., Greige-Gerges H., et al., Protein-Based Nanoparticle Preparation via Nanoprecipitation Method, *Materials (Basel)*, **11**: 394 (2018).

[26] Abdelmoez W., Yoshida H., Simulation of Fast Reactions in Batch Reactors Under Sub-Critical Water Condition, *AIChE J.*, **52**: 3600 (2006).

[27] Bayraktar E., Response Surface Optimization of the Separation of DL-Tryptophan Using An Emulsion Liquid Membrane, *Process Biochem.*, **37**: 169 (2001).

[28] Joye I.J., McClements D.J., Production of Nanoparticles by Anti-Solvent Precipitation for Use in Food Systems, *Trends Food Sci. Technol.*, **34**: 109 (2013).

[29] Langer K., Balthasar S., Vogel V., Dinauer N., von Briesen H., Schubert D., Optimization of the Preparation Process for Human Serum Albumin (HSA) Nanoparticles, *Int. J. Pharm.*, **257**: 169 (2003).

[30] Danaei M., Dehghankhold M., Ataei S., Hasanzadeh Davarani F., Javanmard R., Dokhani A., et al., Impact of Particle Size and Polydispersity Index on the Clinical Applications of Lipidic Nanocarrier Systems, *Pharmaceutics*, 10 (2018).

[31] Hu H., Yang H., Huang P., Cui D., Peng Y., Zhang J., et al., Unique Role of Ionic Liquid In Microwave-Assisted Synthesis of Monodisperse Magnetite Nanoparticles, *Chem. Commun.*, **46**: 3866 (2010).

[32] Huang P., Li Z., Hu H., Cui D., Synthesis and Characterization of Bovine Serum Albumin-Conjugated Copper Sulfide Nanocomposites, *J. Nanomater*, **2010**: 1 (2010).

[33] Naveenraj S., Anandan S., Binding of Serum Albumins with Bioactive Substances – Nanoparticles to Drugs, *J. Photochem. Photobiol. C Photochem. Rev.*, **14**: 53 (2013).

[34] Patra S., Santhosh K., Pabbathi A., Samanta A., Diffusion of Organic Dyes in Bovine Serum Albumin Solution Studied by Fluorescence Correlation Spectroscopy, *RSC Adv.*, **2**: 6079 (2012).

[35] Shi J.-H., Pan D.-Q., Wang X.-X., Liu T.-T., Jiang M., Wang Q., "Characterizing the Binding Interaction Between Antimalarial Artemether (AMT) and Bovine Serum Albumin (BSA): Spectroscopic and Molecular Docking Methods" (2016).

[36] Galisteo-González F., Molina-Bolívar J.A., Systematic Study on the Preparation of BSA Nanoparticles, *Colloids Surf. B Biointerfaces*, **123**: 286 (2014).

[37] Rahimnejad M., Najafpour G., Bakeri G., Investigation and Modeling Effective Parameters Influencing the Size of BSA Protein Nanoparticles as Colloidal Carrier, *Colloids and Surfaces*, 96 (2012).

[38] Santhi K., Dhanaraj S.A., Joseph V., Ponnusankar S., Suresh B., A Study on the Preparation and Anti-Tumor Efficacy of Bovine Serum Albumin Nanospheres Containing 5-Fluorouracil, *Drug. Dev. Ind. Pharm.*, **28**: 1171 (2002).

[39] Wang G., Siggers K., Zhang S., Jiang H., Xu Z., Zernicke R.F., et al., Preparation of BMP-2 Containing Bovine Serum Albumin (BSA) Nanoparticles Stabilized by Polymer Coating, *Pharm. Res.*, **25**: 2896 (2008).

[40] Argast A. and Tennis C.F., A Web Resource f or the Study of Alkali Feldspars and Perthitic Textures Using Light Microscopy, Scanning Electron Microscopy and Energy Dispersive X-Ray Spectroscopy, *J. Geosci. Educ.*, **52**: 213 (2004).

[41] Jahanshahi M., Babaei Z., Protein Nanoparticle: A Unique System as Drug Delivery Vehicles, African *J. Biotechnol.*, **7**: 4926 (2008).

[42] Yeon Jun J., Hai Nguyen H., Paik S.-Y.-R., Sook Chun H., Kang B.-C., Ko S., Preparation of Size-Controlled Bovine Serum Albumin (BSA) Nanoparticles By A Modified Desolvation Method, *Food Chem.*, **127**: 1892 (2011).

[43] Honary S., Zahir F., Effect of Zeta Potential on the Properties of Nano-Drug Delivery Systems - A Review (Part 2), *Trop. J. Pharm. Res.*, **12**: 265 (2013).

[44] SChmidt R.H., "Gelation and Coagulation". In: Cherry J.P., (Editor). Protein Funct. Foods, **147**, American Chemical Society; (1981).

[45] Sun X.D., Holley R.A., Factors Influencing Gel Formation by Myofibrillar Proteins in Muscle Foods, *Compr. Rev. Food Sci. Food Saf.*, **10**: 33 (2011).